Theor. Comput. Fluid Dyn. (2010) 24:315–322
DOI 10.1007/s00162-009-0099-4

ORIGINAL ARTICLE

R. Kunnen · R. Trieling · G. J. van Heijst

Vortices in time-periodic shear flow

Received: 8 January 2009 / Accepted: 18 March 2009 / Published online: 8 May 2009

Abstract Vortices emerging in geophysical turbulence may experience deformations due to the non-uniform ambient flow induced by neighbouring vortices. At first approximation this ambient flow is modeled by a linear shear flow. It is well known from previous studies that the vortex may be (partially) destructed through removal of weak vorticity at the vortex edge—a process referred to as 'stripping'. While most previous studies considered a stationary external shear flow, we have examined the behaviour of the vortex embedded in a linear shear flow whose strength changes harmonically in time. Aspects of the vortex dynamics and the (chaotic) transport of tracers have been studied by both laboratory experiments and numerical simulations based on a simple kinematical model.

Keywords Vortex dynamics · Rotating fluids · Shear flow · Lobe dynamics · Laboratory experiments · Contour kinematics

PACS 47.32.C- · 47.32.F.f

1 Introduction

Background rotation and/or density stratification in a fluid tend to suppress one velocity component, often giving the flow a quasi-two-dimensional (quasi-2D) character. Such conditions are commonly encountered in large-scale geophysical flows. As a result of the inverse energy cascade active in 2D turbulence, such flows (even when quasi-2D) show a tendency of self-organisation, usually observed in the emergence of vortex structures (see e.g. [6]). The vortices of 2D turbulence are embedded in a non-uniform flow field, and hence they generally undergo time-dependent straining deformations. A natural question arising is: how is a vortex affected by the strain imposed by the exterior flow? Only a very few analytical studies have been carried out for vortices in a strain or shear flow: the case of steady vortex patches in a linear shear flow was studied by Moore and Saffman [10], while this work was extended by Kida [4] to include unsteady solutions. In fact, work on this topic was also carried out by S. A. Chaplygin and published (in Russian) already in 1899, see the review by Meleshko and van Heijst [8]. Much later, Legras and Dritschel [5] performed a numerical study of the behaviour of nested patches of uniform vorticity in a shear flow by using the method of contour dynamics. In experimental studies on 2D vortices one often applies background rotation, see the recent review by van Heijst and Clercx [3]. In this line of approach Trieling et al. [16] performed an experimental study of a single vortex in an annular shear flow. While most previous studies were aimed at vortices in a steady strain/shear flow, in the present paper we will focus on time-dependent external shear flow. In order to study the tracer transport in such unsteady flows we introduce an extremely simple kinematical model of the flow, consisting of a point

Communicated by H. Aref

R. Kunnen · R. Trieling · G. J. van Heijst (✉)
Fluid Dynamics Laboratory, Department of Physics, Eindhoven University of Technology, Eindhoven, The Netherlands
E-mail: g.j.f.v.heijst@tue.nl

vortex of constant strength placed in a linear shear flow whose amplitude is perturbed harmonically. Such an approach was also used by Perrot and Carton [13,14] in their study of vortex interactions in an unsteady ambient shear flow. In fact, this approach is closely related to earlier studies by Rom-Kedar et al. [15] and Velasco Fuentes et al. [17,18] on modulated point vortices, in which the vortex strength was made (or allowed) to be time dependent. In addition, a laboratory experiment is carried out in a rectangular fluid tank rotating about its vertical axis. A cyclonic vortex is generated by siphoning, while the time-periodic shear flow is produced by a modulation of the rotation speed of the turntable. The model results show very good agreement with the dye-visualised vortex flow. The kinematical model and the technique of the numerical computations based on it will be briefly reviewed in Sect. 2, while the experimental arrangement and the flow visualization results will be described in Sect. 3. The main conclusions will be drawn in Sect. 4.

2 Theoretical model

The trajectory $(x(t), y(t))$ of a fluid particle in an incompressible two-dimensional flow can be described by the following equations:

$$\frac{\mathrm{d}x}{\mathrm{d}t} = \frac{\partial \Psi}{\partial y}, \quad \frac{\mathrm{d}y}{\mathrm{d}t} = -\frac{\partial \Psi}{\partial x}, \tag{1}$$

where Ψ is the stream function. We can interpret (1) as a Hamiltonian system with Hamiltonian function Ψ. If Ψ is independent of time this Hamiltonian system has one degree of freedom, while for time-dependent Ψ it has two degrees of freedom. When Ψ is periodic in time this system is said to have 'one and a half' degrees of freedom [11]. The dynamics of systems of various degrees of freedom differ considerably. In steady, one-degree-of-freedom flows only linear dynamics can occur. Aref [1] showed that time-periodic flows can produce chaotic particle paths, thus enabling complicated fluid mixing in these flows.

The stream function of the flow induced by a point vortex in a linear shear flow is

$$\Psi = \frac{1}{2}\alpha_0 y^2 - \frac{\gamma}{4\pi}\ln(x^2 + y^2), \tag{2}$$

with α_0 the shear strength and γ the strength of the point vortex. For the remainder of this section we restrict ourselves to positive values of α_0 and γ. In that case there exist two stagnation points $\mathbf{p}_\pm$ at $(0, \pm\sqrt{\gamma/2\pi\alpha_0})$ in the flow. We denote this characteristic radius by $r_p = \sqrt{\gamma/2\pi\alpha_0}$. The corresponding streamline pattern is shown in Fig. 1a. The dotted streamlines divide the flow into several separate regions; therefore they are known as separatrices.

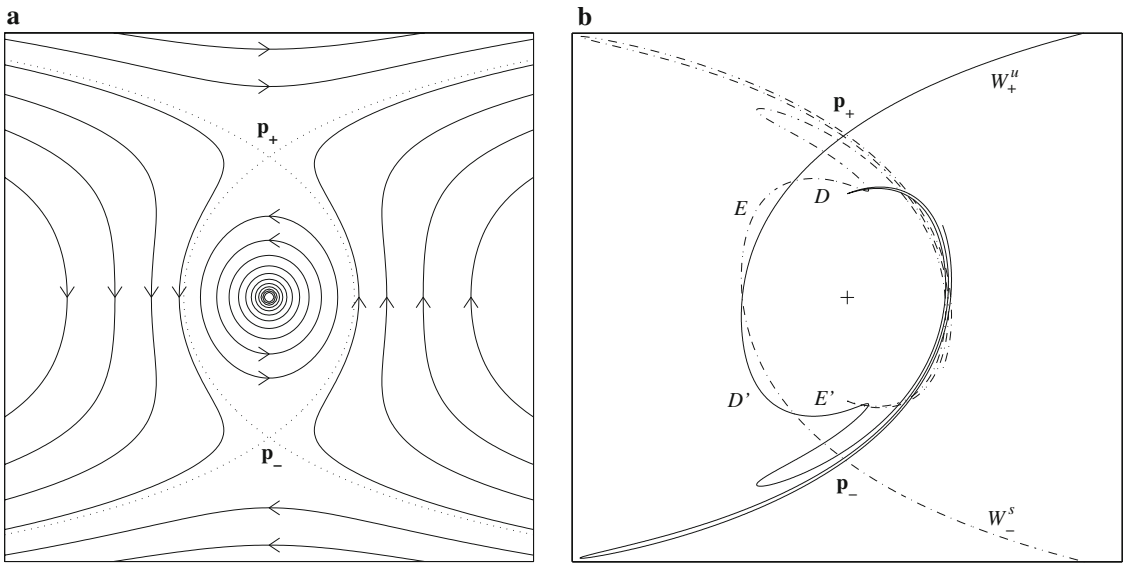

Fig. 1 **a** Streamline pattern of the flow due to a point vortex in an unperturbed linear shear flow. The hyperbolic points are indicated by $\mathbf{p}_+$ and $\mathbf{p}_-$. **b** In the perturbed case, the unstable manifold W^u_+ of $\mathbf{p}_+$ intersects with the stable manifold W^s_- of $\mathbf{p}_-$. The intersection of W^s_+ and W^u_- is omitted here for clarity. The symbols D, D', E, and E' indicate detrainment and entrainment lobes

The behaviour of this Hamiltonian system changes drastically when a perturbation is introduced. Here we insert a small harmonic variation in the shear strength α

$$\alpha(t) = \alpha_0[1 + \epsilon \cos(\omega_p t)], \tag{3}$$

in which α_0 is the basic-state shear strength, ϵ is the (small) amplitude of perturbation, and ω_p is the perturbation frequency. We can now non-dimensionalise the stream function with $\tilde{\mathbf{x}} = \mathbf{x}/r_p$, $\tilde{t} = \alpha_0 t$, and $\tilde{\Psi} = \Psi/\alpha_0 r_p^2$:

$$\tilde{\Psi} = \frac{1}{2}\tilde{y}^2 \left[1 + \epsilon \cos\left(\frac{\omega_p}{\alpha_0}\tilde{t}\right)\right] - \frac{1}{2}\ln(\tilde{x}^2 + \tilde{y}^2). \tag{4}$$

(The scaling of the logarithmic term is accounted for in the arbitrary constant that can always be added to a stream function.) Henceforth we drop the tildes for convenience. Two dimensionless numbers determine the flow: (i) the perturbation amplitude ϵ, and (ii) the ratio of ω_p and α_0, which we will from now on refer to as the timescale ratio $\sigma = \omega_p/\alpha_0$. The equations of motion (1) thus become

$$\begin{aligned} \frac{\mathrm{d}x}{\mathrm{d}t} &= y[1 + \epsilon \cos(\sigma t)] - \frac{y}{x^2 + y^2}, \\ \frac{\mathrm{d}y}{\mathrm{d}t} &= \frac{x}{x^2 + y^2}. \end{aligned} \tag{5}$$

When the trajectory of a given particle with initial position $\mathbf{X}$ is given by the function $\Phi_t(\mathbf{X})$ for all t, we can introduce a Poincaré mapping F for the periodic flow as

$$\mathbf{x}_{n+1} = F(\mathbf{x}_n) = \Phi_T(\mathbf{x}_n), \tag{6}$$

with $\mathbf{x}_n$ the position of a particle after a time nT, and T being the period of perturbation. The stable and unstable manifolds W^s and W^u of a hyperbolic point $\mathbf{p}$ are defined as

$$\begin{aligned} W^s(\mathbf{p}) &= \{\forall\, \mathbf{X} \in \mathbb{R}^N | F(\mathbf{X}) \to \mathbf{p} \Leftrightarrow t \to \infty\}, \\ W^u(\mathbf{p}) &= \{\forall\, \mathbf{X} \in \mathbb{R}^N | F(\mathbf{X}) \to \mathbf{p} \Leftrightarrow t \to -\infty\}. \end{aligned} \tag{7}$$

Under perturbation the separatrices degrade to a structure of intersecting stable and unstable manifolds of the hyperbolic points, called the heteroclinic tangle, see Fig. 1b. The hyperbolic points, however, remain as fixed points of the Poincaré map. In the heteroclinic tangle the stable and unstable manifolds enclose so-called lobes. The lobes display the fluid exchange between the interior region and the exterior flow, across the previously impervious separatrices. For a detailed treatment of lobe dynamics, see e.g. Wiggins [19].

The locally chaotic character of the transport induced by this time-dependent flow system is nicely illustrated by the Poincaré map presented in Fig. 2. This map shows the positions of 2 × 1,631 tracer particles initially positioned in the entrainment lobes near the hyperbolic points, after 50 cycles of the harmonic perturbation. One clearly observes three 'empty' regions, in which no particles have penetrated: one central region, in which no particles can penetrate due to the elliptic nature of the vortex core, and two curved, elongated regions on either side of the elliptical central region. The distribution of the particles clearly reveals the entrainment near the hyperbolic points in the form of lobes that become very elongated when closer to the hyperbolic points. Calculations with different perturbation frequencies ω_p have revealed that for higher frequencies the size of the empty central region increases, while the dispersion band of the tracer particles becomes narrower. Also, the lobes become more elongated and narrower, while covering a decreasing area for increasing frequency.

Melnikov [9] derived an analytical technique that measures the distance between the stable and unstable manifolds for small perturbation amplitudes. This expression is now known as the Melnikov function. Using this function one can calculate the area of a lobe, and hence derive a quantity that provides a measure of the net exchange of mass between the vortex and its exterior. In order to study the transport properties of the perturbed vortex for larger perturbation amplitudes, we adopted the so-called contour kinematics method, which monitors in time a contour defined by passive markers connected by small line segments. When sufficient markers are used, the contour appears smooth. Initially the markers form a circle. Integrating the advection equation (1) for each marker results in the evolution of the contour in time. The contour will get stretched and folded by the

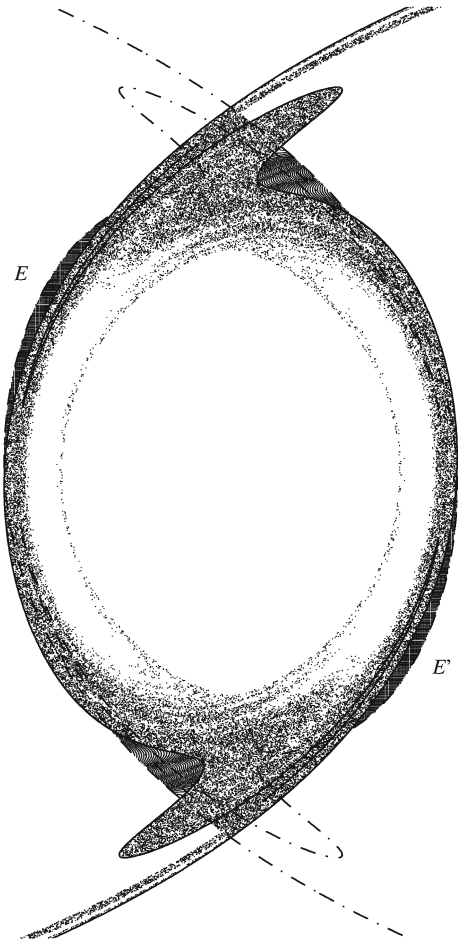

Fig. 2 Poincaré map showing the positions of 2 × 1,631 passive tracer particles, initially placed in the entrainment lobes close to the hyperbolic points, after 50 cycles of the perturbation. Perturbation frequency 1.6π

flow. All time integrations are performed using a variable-order Runge–Kutta scheme. The contour kinematics method has been tested extensively, and for a more detailed description, the reader is referred to Meleshko and van Heijst [7]. The mechanism of stretching and folding, clearly present near the hyperbolic points, see Fig. 1b, leads to rapid distortions of closed material contours released close to these points. This effect has been investigated by monitoring the length stretch of a contour initially placed around the fixed point $\mathbf{p}_+$ for different values of the frequency $f_s = \omega_p/2\pi$. The length stretch λ is defined as $\lambda = l(t)/l(0)$, where $l(t)$ is the contour length at time t and $l(0)$ is the initial length at $t = 0$. The results of the calculations are shown in Fig. 3. At first, one observes an exponential stretch when the contour is still near the hyperbolic point. From $t = 2.5$ onwards, the contour stretch is different for different frequencies. The broken line represents the unperturbed case, in which the contour length increases linearly. In the perturbed case, however, fluid particles may separate at an exponential rate. The stretch curves for $t > 2.5$ are roughly linear, thus revealing exponential stretching. For higher perturbation frequencies f_s, the stretching and folding mechanism active near the stagnation points is more effective and results in enhanced stretching of the contours, as visible in the steeper slopes of the stretch curves in Fig. 3.

3 Laboratory experiments

3.1 Description of the experimental set-up

The experiments were performed in a rectangular plexiglass tank of dimensions length × width × height = 200 × 40 × 30 cm. This tank was mounted on a turntable, centred on the axis of rotation. It was filled with

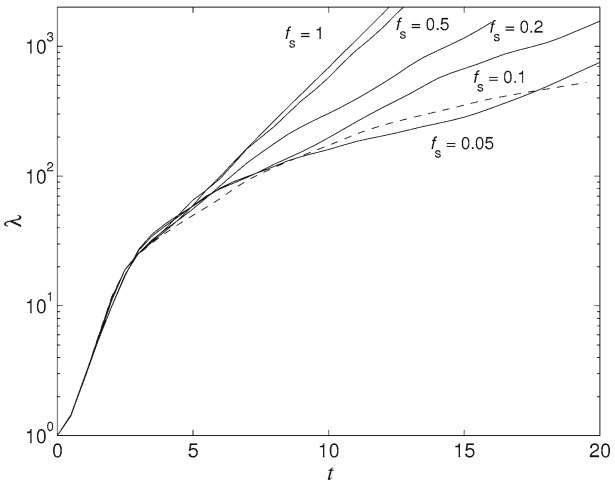

Fig. 3 Length stretch $l(t)/l(0)$ of a contour initially placed around the fixed point $\mathbf{p}_+$. The *broken line* represents the unperturbed case ($\varepsilon = 0$). The *solid lines* represent perturbed cases, for different values of the frequency f_s. Other parameter values: $\gamma = 8\pi,\ a_0 = 1,\ \varepsilon = 0.1$

water to a depth of $H = 20\,\text{cm}$. A co-rotating camera was mounted about 1 m above the water surface. A perforated plexiglass tube with 32 holes, distributed uniformly over a length of 15 cm, was placed vertically along the axis of rotation.

By virtue of the Taylor–Proudman theorem (see e.g. [12]), rotation causes the flow in the tank to behave as a two-dimensional flow. Furthermore, a vortex can be generated under rotation by siphoning fluid through the perforated tube. The inward flow towards the tube is deflected by the Coriolis force, resulting in a cyclonic vortex. The circulation Γ of this vortex is given by

$$\frac{D\Gamma}{Dt} = -2\oint_C (\mathbf{\Omega} \times \mathbf{v}) \cdot \mathrm{d}\mathbf{s} = -\frac{2\Omega q}{H}, \tag{8}$$

with D/Dt the material derivative, C a material contour enclosing the sink tube, $\mathbf{\Omega}$ the rotation vector, $d\mathbf{s}$ an infinitesimal segment of C, and q the (negative) volume flux.

An instantaneous increase of the rotation speed of the tank leaves the fluid lagging behind, and thus an anticyclonic flow is observed in a co-rotating frame of reference. van Heijst et al. [2] studied the spin-up process and the resulting flow in the rotating frame. When using a large-aspect-ratio tank this flow creates to very good approximation a linear shear in the central region of the tank. The magnitude of the shear constant α is then equal to twice the value of the change in rotation velocity $\Delta\Omega$. Oscillations of the shear are made by constantly changing the computer-controlled rotation speed of the turntable. The anticyclonic flow enacted by a stepwise change of Ω is dampened through Ekman dynamics. The characteristic timescale associated with this process is the so-called Ekman decay time $T_E = H/(\nu\Omega)^{1/2}$, with ν being the kinematic viscosity. An experiment in such a shear flow should therefore preferably be finished well within this time. In our experiments T_E was typically 240 s.

Qualitative experiments were performed in which the flow was visualised with a fluorescent dye. The dye, a passive tracer, is evidently suitable for visualisation of the unstable manifolds of the hyperbolic points. A blob of dye released around a hyperbolic point will be advected away from this point along the unstable manifold, thereby marking it. Quantitative experiments were also performed (by using a high-resolution combined PIV–PTV technique), but the results of these will be reported elsewhere.

3.2 Results

In order to obtain qualitative information about the evolution of the vortex in the perturbed shear flow, dye visualization experiments were carried out. In one particular series of experiments a small blob of fluorescent dye was introduced at the free surface of the fluid, near one of the stagnation points in the flow. The evolution of the dye pattern was recorded from above by a co-rotating camera. Four snapshots of this dye-visualised experiment are displayed in Fig. 4 (left column), on which the structure of the unstable manifolds is clearly visible. In

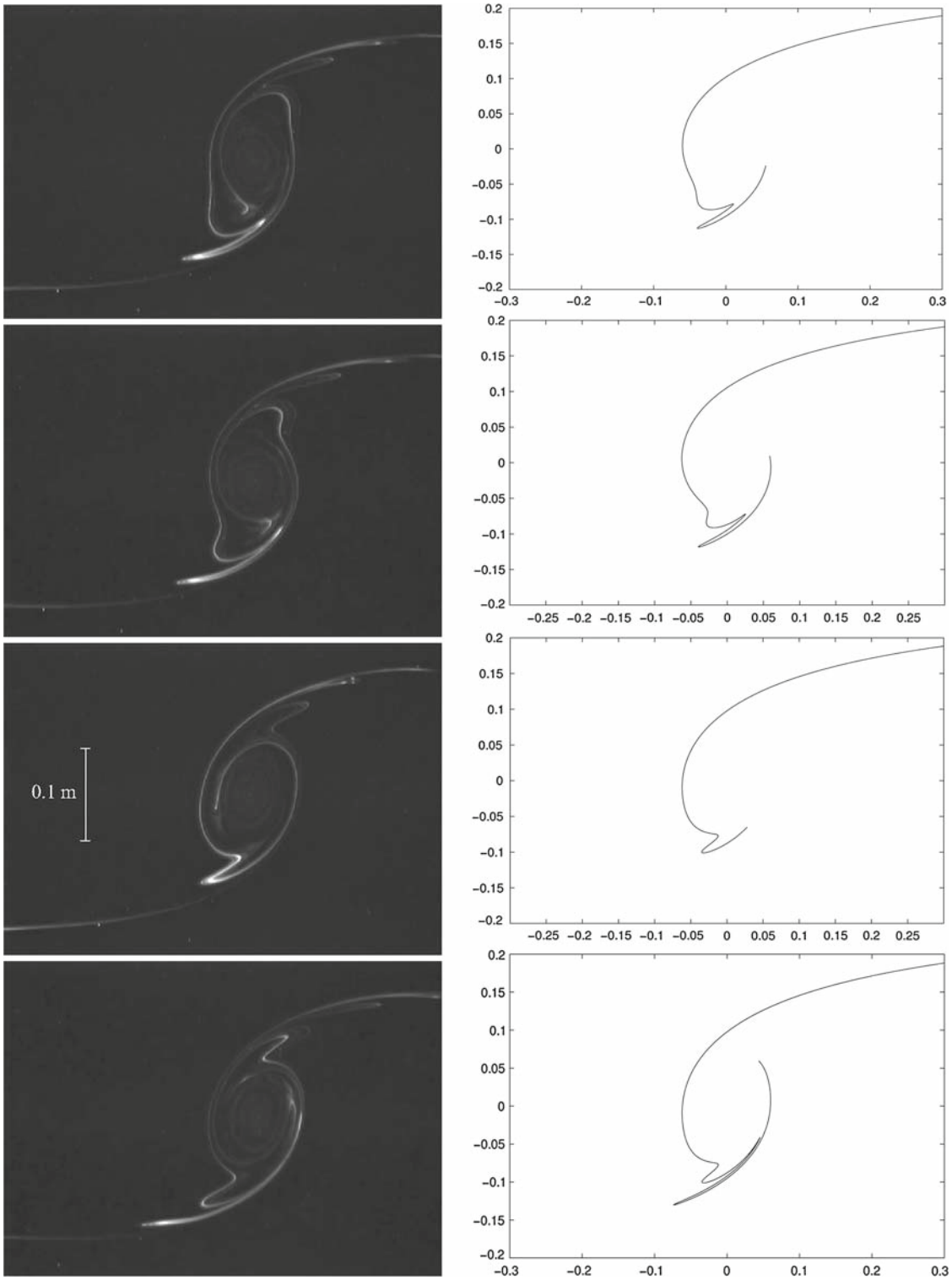

Fig. 4 Time evolution of the vortex in an oscillating shear flow: dye visualization in the laboratory experiment (*left column*), numerical contour kinematics simulation (*right column*). The snapshots correspond with $t/T = 0,\ 0.4,\ 0.6,\ 1.0$ and thus span a full perturbation period T. Parameter values: $\Omega = 0.7\,\mathrm{rad\,s^{-1}}$, $\Delta\Omega = 0.05\,\mathrm{rad\,s^{-1}}$, $\Gamma = 6.3 \times 10^{-3}\,\mathrm{m^2 s^{-1}}$, $\epsilon = 0.4$, $f_s = 0.1\,\mathrm{s^{-1}}$ (in the numerical simulation: $\gamma_0 = 6.3 \times 10^{-3}$, $\alpha_0 = 0.1$, $f_s = 0.1$, $\varepsilon = 0.4$)

particular one observes the process of repeated stretching and folding taking place near the stagnation points. Furthermore, the lobes are elongated along the unstable manifolds of the hyperbolic points, and hence leaving the vortex region. It is instructive to make a comparison with the plot of the unstable manifolds, see Fig. 1b.

Additionally, see Fig. 4 (right column), a contour kinematics simulation was made for the same flow conditions, with the initial, circular contour placed around the upper stagnation point. It is obvious that the distortion of the contour is very similar to the dye patterns observed in the experiment: even the details of the repeated stretching and folding near the lower stagnation point seem to be well captured by the contour kinematics simulations. This stresses the value of this simple kinematical flow model, based on a potential vortex. An equally good agreement between experimental dye-visualisations and a (modulated) point-vortex model was obtained by Velasco Fuentes et al. [17,18] in their studies of topography-perturbed dipolar and tripolar vortices.

A very careful comparison between the dye visualization and the contour kinematics simulations reveals a few small differences, however: the dye visualizations indicate that the stagnation points are not exactly positioned on a line perpendicular to the basic shear flow direction, while in the kinematical model they are (by definition). The explanation lies in the continuous, finite-sized vorticity distribution present in the 'real' flow, i.e. in the laboratory experiment. Hence, the shape of the vorticity distribution may change during the experiment and besides, the vortex is continuously eroded by stripping of low-amplitude vorticity at its edge. As a result, the experimental vortex shrinks and decays in the course of the experiment, while that of the kinematical model has a fixed strength. Of course, such effects may also be incorporated in the model, but this lies beyond the scope of the present paper.

4 Conclusion

The behaviour of tracer transport due to a vortex in a time-periodic shear flow was modeled in the simplest possible way, viz. by a point vortex in a harmonically perturbed linear shear flow. The two stagnation points appearing in this flow play a key role in the tracer transport: the intersecting stable and unstable manifolds show lobes, the area of which is directly related to entrainment/detrainment between the vortex interior and exterior. For small perturbation amplitudes the lobe area—and hence the exchange rate of material—can be determined by using Melnikov's theory. For larger amplitudes, one is forced to use numerical techniques like the contour kinematics method. Simulations with an initially circular contour placed around one of the hyperbolic points show the rapid advection away from this point and the subsequent substantial deformation when reaching the other stagnation point. Such contour advection simulations nicely reveal the stretching and folding mechanism present near the stagnation points in the perturbed flow. The length stretch of the contour is found to behave exponentially in time, the growth rate increasing with higher frequency.

A laboratory experiment has been performed in which the transport properties of the sheared vortex were studied qualitatively. The vortex flow was created in a homogeneous fluid contained in a long rectangular tank rotating about its vertical axis by removing some fluid by siphoning. A shear flow could be established for some time in the central part of the tank by accelerating or decelerating the rotating table slightly. By adding a sinusoidal modulation on top of this increased or decreased rotation speed, the shear flow was perturbed harmonically. The resulting flow was visualized by locally adding neutrally buoyant dye to the fluid. When introduced near one of the stagnation points, the evolution of the dye patch clearly shows the repeated stretching and folding taking place near the stagnation points, thus visualizing the structure of the stable and unstable manifolds.

The agreement between the contour kinematics simulations based on the simple point-vortex model and the visualized flow in the laboratory experiment illustrates how powerful such a simple kinematical model may be for the purpose of describing tracer transport.

References

1. Aref, H.: Stirring by chaotic advection. J. Fluid Mech. **143**, 1–21 (1984)
2. van Heijst, G.J.F., Davies, P.A., Davis, R.G.: Spin-up in a rectangular container. Phys. Fluids A **2**, 150–159 (1990)

3. van Heijst, G.J.F., Clercx, H.J.H.: Laboratory modelling of geophysical vortices. Annu. Rev. Fluid Mech. **41**, 143–164 (2009)
4. Kida, S.: Motion of an elliptic vortex in a uniform shear flow. J. Phys. Soc. Jpn **50**, 3517–3520 (1981)
5. Legras, B., Dritschel, D.G.: Vortex stripping and the generation of high vorticity gradients in two-dimensional flows. Appl. Sci. Res. **51**, 445–455 (1993)
6. McWilliams, J.C.: The emergence of isolated, coherent vortices in turbulent flow. J. Fluid Mech. **146**, 21–43 (1984)
7. Meleshko, V.V., van Heijst, G.J.F.: Interacting two-dimensional vortex structures: point vortices, contour kinematics and stirring properties. Chaos Solitons Fractals **4**, 977–1010 (1994)
8. Meleshko, V.V., van Heijst, G.J.F.: On Chaplygin's investigations of two-dimensional vortex structures in an inviscid fluid. J. Fluid Mech. **272**, 157–182 (1994)
9. Melnikov, V.K.: On the stability of the center for time periodic perturbations. Trans. Moscow Math. Soc. **12**, 1–57 (1963)
10. Moore, D.W., Saffman, P.G.: Structure of a line vortex in an imposed strain. In: Olsen, J.H., Goldburg, A., Rogers, M. (eds.) Aircraft Wake Turbulence and its Detection, pp. 339–354 (1971)
11. Ottino, J.M.: The Kinematics of Mixing: Stretching, Chaos and Transport. Cambridge University Press, London (1989)
12. Pedlosky, J.: Geophysical Fluid Dynamics. Springer, Heidelberg (1979)
13. Perrot, X., Carton, X.: Vortex interaction in an unsteady large-scale shear/strain flow. In: Borisov, A.V., Kozlov, V.V., Mamaev, I.S., Sokolovskiy, M.A. (eds.) Proceedings IUTAM Symposium on Hamiltonian Dynamics, Vortex Structures, Turbulence, pp. 373–381. Springer, Heidelberg (2008)
14. Perrot, X., Carton, X.: Point-vortex interaction in an oscillatory deformation field: Hamiltonian dynamics, harmonic resonance and transition to chaos. Discr. Cont. Dyn. Syst. Ser. B **11**, 971–995 (2009)
15. Rom-Kedar, V., Leonard, A., Wiggins, S.: An analytical study of transport, mixing and chaos in an unsteady vortical flow. J. Fluid Mech. **214**, 347–394 (1990)
16. Trieling, R.R., Linssen, A.H., van Heijst, G.J.F.: Monopolar vortices in an irrotational annular shear flow. J. Fluid Mech. **360**, 273–294 (1998)
17. Velasco Fuentes, O.U., van Heijst, G.J.F., Cremers, B.E.: Chaotic transport by dipolar vortices on a β-plane. J. Fluid Mech. **291**, 139–161 (1995)
18. Velasco Fuentes, O.U., van Heijst, G.J.F., van Lipzig, N.P.M.: Unsteady behaviour of a topography-modulated tripole. J. Fluid Mech. **307**, 11–41 (1996)
19. Wiggins, S.: Introduction to Applied Nonlinear Dynamical Systems and Chaos. Springer, Heidelberg (1990)